International Journal of Scientific Advances
ISSN: 2708-7972
Volume: 2 | Issue: 3 | May - Jun 2021 Available Online: www.ijscia.com
DOI: 10.51542/ijscia.v2i3.18

Synthesis and Antibacterial Effect Evaluation of AgNPs, TiO_2NPs, and TiO_2-Ag Nanocomposites

Mourad Chkaif [1,2]

[1]College of Environmental Science and Engineering, Biomedical Multidisciplinary Innovation Research Institute, Shanghai East Hospital, Tongji University Shanghai 200092, China

[2]UN Environment-Tongji Institute of Environment for Sustainable Development (IESD) Tongji University, Shanghai 200092, China

Corresponding author details: Mourad Chkaif; 1993241@tongji.edu.cn

ABSTRACT

Due to the increase of bacterial infections that keep threatening human health and safety, the need for efficient and strong antibacterial agents is still fatal. TiO_2 nanoparticle's photocatalytic properties have been widely used as antibacterial agents. However, the use of this photocatalytic nanomaterial has some drawbacks due to its wide bandgap energy and necessity for UV irradiations. TiO_2-Ag nanocomposite has been recognized as one of the good bactericidal agents due to its excellent antibacterial and photocatalytic properties upon visible light. To explore the antibacterial activity of these nanomaterials, this study was conducted to synthesize three types of nanomaterials, namely silver nanoparticles (AgNPs), titanium dioxide nanoparticles (TiO_2), and TiO_2-Ag nanocomposites. TiO_2 was doped with carbon and nitrogen elements (C,N-TiO_2) in this study to improve the photocatalytic activity of TiO_2 under visible light irradiation. C,N-TiO_2 was further used to combine with AgNPs to form a novel nanocomposite (TiO_2-Ag). Both SEM and TEM techniques were used to characterize the nanomaterials' morphology and size. The nanoparticles' crystalline phase was further investigated via the XRD technique. The antibacterial effect of the synthesized nanoparticles within the concentration range of 10, 20, 50, and 100 ppm was tested using two different strains of bacteria, i.e., E. coli and B. subtilis.
The C,N-TiO_2-Ag showed a better antibacterial effect against both bacterial strains compared AgNPs and C,N-TiO_2 nanoparticles.

Keywords: antibacterial; nanocomposite; AgNPs; C,N-TiO_2; C,N-TiO_2-Ag

INTRODUCTION

In recent years, bacterial infections increased intensely and continue to be a major threat to human health [1]. Consequently, there is a crucial need for new antibacterial agents to overcome the ever-increasing bacterial infections [2]. In such a scenario, nanomaterials such as titanium dioxide (TiO_2) and silver (Ag) are an active area of research nowadays [3][4]. Titanium dioxide nanoparticle is a semiconductor nanomaterial that has been widely used in environmental utilizations such as in water treatment and disinfection, air purification, and food packaging industry, due to its excellent photocatalytic effect, chemical stability, it has shown great antibacterial activity against a wide range of bacteria [5]. It has three principal crystalline structures; Anatase, Rutile, and Brookite [6] [7]. However, the large bandgap of TiO_2 (~3.2 eV) and the fast electron-hole recombination properties remain a hindrance that limits the photocatalytic antibacterial performance of TiO_2 as it can only be activated upon the UV energy of the solar spectrum [8] [9]. Due to this wide-bandgap of the TiO_2 and the necessity of UV light irradiation to activate it, the photocatalytic activity of titanium dioxide nanoparticles must be further improved for more practical utilizations in the future as an antibacterial agent.

An effective method is to modify the TiO_2 by combine it with one or multiple metals or metal oxides on its matrices. The combination with noble metal nanoparticles can extend the light absorption range and improve the solar energy's utilization efficiency[10]. Undeniably, the photocatalytic reactions' proficiency is determined by the high recombination rate of photoinduced electron-hole pairs generated during the photocatalytic procedures and by the absorption ability for visible light [11]. Among various noble metals, AgNPs have received much attention for this purpose. However, before anything, silver itself is known as one of the strongest antibacterial materials for decades [12]. Silver nanoparticles have been identified with their high thermal stability and great antibacterial activity against a wide range of bacteria [13] [14]. Silver is a suitable and nontoxic element that improves the TiO_2 bioactivity because of its inborn antibacterial activity against different microorganisms [15]. Silver nanoparticles have shown an excellent ability to enhance the photocatalytic activity of TiO_2 in the visible light region [16]. Therefore, TiO_2-Ag is one of the excellent nanocomposites that can be used as an antibacterial agent against a broad range of bacteria under solar light irradiation [17].

This study was conducted to synthesize three types of nanomaterials, namely silver nanoparticles (AgNPs), titanium dioxide nanoparticles (TiO_2), and TiO_2-Ag nanocomposites. TiO_2 was doped with carbon and nitrogen elements (C,N-TiO_2) in this study to improve the photocatalytic activity of TiO_2 under visible light irradiation. C,N-TiO_2 was further used to combine with AgNPs to form a novel nanocomposite TiO_2-Ag. These nanoparticles were investigated via SEM, TEM, and XRD techniques. Furthermore, their antibacterial activity was also investigated against both gram-negative (E. coli) and gram-positive (B. subtilis) bacteria1.

MATERIALS AND METHODS

1) Silver Nanoparticles (AgNPs) Synthesis

First of all, three solutions were prepared; silver nitrate (100 mg + 10 ml distilled water), $NaBH_4$ (10 mg + 10 ml DI water), and Trisodium (500 mg + 50 ml DI). These solutions were used to synthesize silver seeds with a size of around 4 nm. For that, 20 ml of trisodium solution was added to 70 ml of DI water in a round bottom flask under 70 °C for 15 min. Then, 1.7 ml of silver nitrate ($AgNO_3$) and 2 ml of $NaBH_4$ were added simultaneously under the heating at 70 °C for one hour. Then we get the silver seeds nanoparticles of around 4 nm in size. This solution was purified for 12 hours using a biological membrane.

To synthesizing silver solution with 20 nm of size, the seeds solution of 4 nm was used. For that matter, 2 ml of Trisodium solution was added to 80 ml of DI water and put into the round bottom flask under heating till it achieves 100 °C for 15 min, then 1.7 ml of seeds solution (4 nm) was added to the solution and 1.7 ml of silver nitrate ($AgNO_3$) followed by a stirred heating for one hour.

2) Carbon, Nitrogen-doped Titanium Dioxide (C,N-TiO_2) Synthesis

The synthesis was done using the same method to synthesize the C,N-TiO2 nanoparticles with some simple modifications. Briefly, 0.2101g of citric acid ($C_6H_8O_7$) and 80µl of perchloric acid ($HClO_4$) were added to 3.6ml of distilled water and then added 0.8250ml of $Ti(NO_3)_4Cl$ (2ml of HNO_3 + 1.25 ml $TiCl_4$ until the color changes to orange). The solution was poured into a small closed bottle under heating of 80 °C for 5 hours. Then the bottle was opened and let under the same heating temperature for 7 hours. After that, the powder was grinded and annealed for 2 hours under 450 °C, 5°C/min.

3) C,N-TiO_2-Ag Nanocomposite Synthesis

The synthesis was done using the same method to synthesize the C,N-TiO_2 nanoparticles with some simple modifications. Briefly, 0.2101g of citric acid ($C_6H_8O_7$) and 80µl of perchloric acid ($HClO_4$) were added to (3ml of distilled water and 0.6ml of AgNPs), then 0.8255ml of $Ti(NO_3)_4Cl$ (2ml of HNO_3 + 1.25ml $TiCl_4$ into a cold environment until the color changes to orange) were added. The solution was poured into a small bottle under heating of 80 °C for 5 hours, and then the bottle was opened and let under the same heating temperature for 7 hours. Then, the powder was grinded and annealed for 2 hours under 450 °C, 5°C/min.

4) Antibacterial Activity Assessment:

This study's targeted microorganisms are gram-negative bacteria (E. coli) and a gram-positive bacterium (B. subtilis). All bacterial tests were done in triplicates and held in 96 well-plates; three wells were used for each solution. Five different nanomaterial solution concentrations were prepared to be used in the antibacterial tests (10, 20, 50, 100ppm). In each well, we used 40µl of the bacterial solution, 80µl of LB, and 80µl of nanomaterial solution (For the control wells, we used PBS solution instead of the nanomaterial solution). The 96-well plates were shacked for 2 min and then transferred into a shaker for incubation at 37 °C for 24 h under continuous light irradiation. The plates were collected after 24 hours of incubation, then the optical density (OD_{600}) was measured as shown in (figure 1). The inhibition rate (IR) was calculated according to the following formula:

$$IR\ (\%) = ((N1-N2)/N1) \times 100\%$$

where N_1 indicates the bacterial concentration of the control solution and N_2 represents the bacterial concentration solution after exposure to the nanoparticles. All the experiments were repeated in triplicates and control experiments were conducted in parallel without nanoparticles.

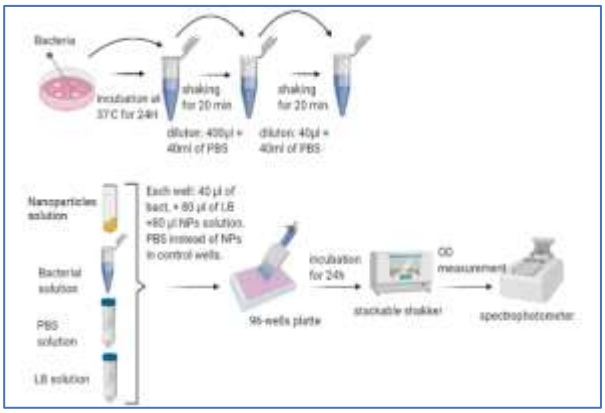

FIGURE 1: experimental design of the antibacterial activity procedure

RESULTS AND DISCUSSIONS

1) Characterization of Nanoparticles

The synthesized products (Ag, C,N-TiO_2, and C,N-TiO_2-Ag nanocomposite) were characterized using transmission electron microscopy (TEM), scanning electron microscopy (SEM) to obtain information about their size and morphology. The X-Ray Diffraction (XRD) technique investigates their crystallographic structure, chemical composition, and physical properties.

- **Silver Nanoparticles' Characterizations**

Practically, the reproducible synthesis of silver nanoparticles in the laboratory was more difficult than expected. This difficulty of synthesis can be related to the initially formed nuclei of metallic silver, which changes into different crystal sizes and morphologies when the reaction conditions (concentrations, reduction agent, temperature, and presence of additive, etc.) are altered [18]. The synthesized silver nanoparticles by reducing silver nitrate can be easily monitored during the reaction from the reaction mixture's change in color. The Silver nanoparticles bear a yellow to brown color due to the HNO_3 reduction, which indicated the formation of silver nanoparticles. Herein, the Samples were characterized and investigated via transmission electron microscopy (TEM). The characterization images show that the silver nanoparticles have a size range of 4~20nm. The TEM characterization images show that the nanoparticles' shape has a spherical shape (figure 2). Also, the scanning electron microscopy (SEM) technique was used in this study to analyze the surface morphology of AgNPs. The SEM images of silver nanoparticles have also shown in (figure 3), which have indicated that morphologically the silver nanoparticles are spherical as well as rod-like of various sizes. The amount of $AgNO_3$ in the reaction mixture and temperature of the reaction was essential in the nanoparticles' size and dispersity.

For those nanoparticles prepared at lower AgNO3 concentrations and temperature, the size distributions of the produced silver nanoparticles are in wide ranges from 5 to 10 nm. For those prepared using higher temperatures and concentrations, their size was found to be around 20 nm. Therefore, it can be concluded based on the results that the size and size distribution of Ag nanoparticles can be controlled by varying the initial $AgNO_3$ concentrations and the temperature of the reaction.

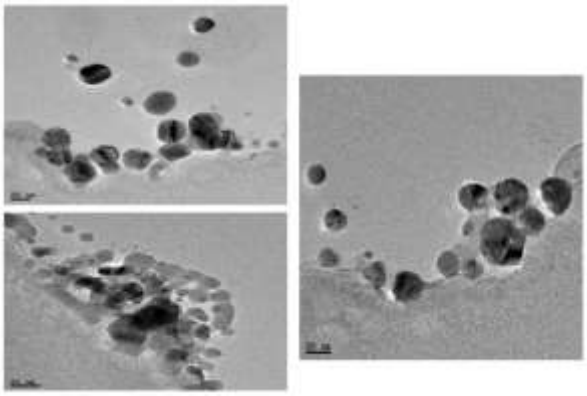

FIGURE 2: TEM characterizations of synthesized silver (AgNPs) nanoparticles.

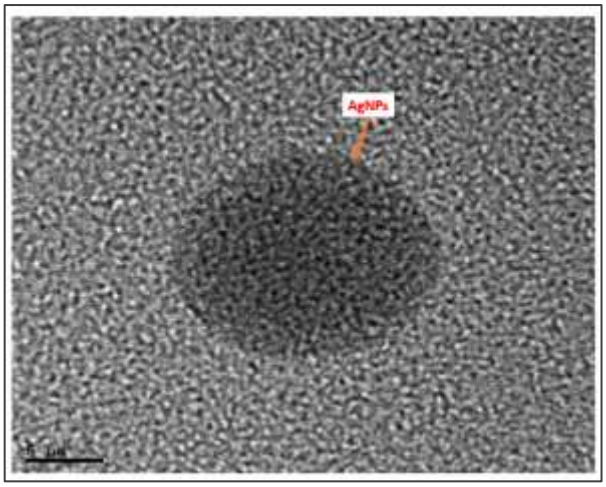

FIGURE 3: SEM characterizations of synthesized silver (Ag) nanoparticles.

• Carbon, Nitrogen-doped Titanium Dioxide Nanoparticles' Characterizations

The surface morphology and size of the C,N-TiO_2 nanoparticles were examined using scanning electron microscopy (SEM), which revealed that C,N-TiO_2 nanoparticles have lamellar layers, each layer has 20~100 nm of thickness. Their size is ranged from 20 to 100 nm (figure 4). The produced nanoparticles were also characterized by transmission electronic microscopy (TEM) (figure 5). The images for C,N-TiO_2 showed that the average size is about 100 nm and has thin lamellar layers. It became evident that the metals used to dope the matrix (titanium dioxide) generally form a crystalline nanoparticle in it, which reveals that the ideal combination of these components yields to the lamellar and porous structures of the synthesized nanocomposite. Without any purification processes, the as-prepared C,N-TiO_2 showed consistent structural features in all views under SEM characterization.

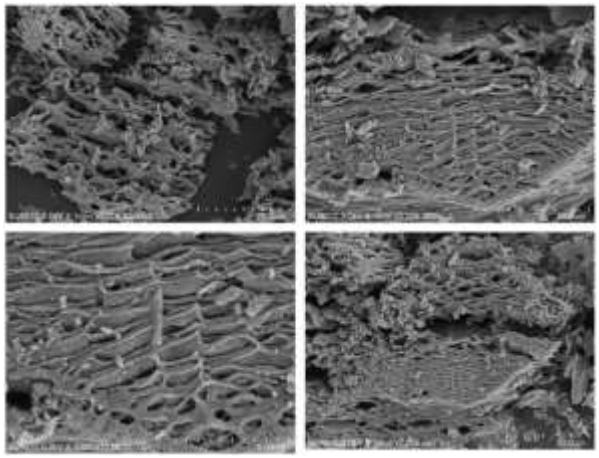

FIGURE 4: SEM characterizations of synthesized C,N-TiO_2 NPs.

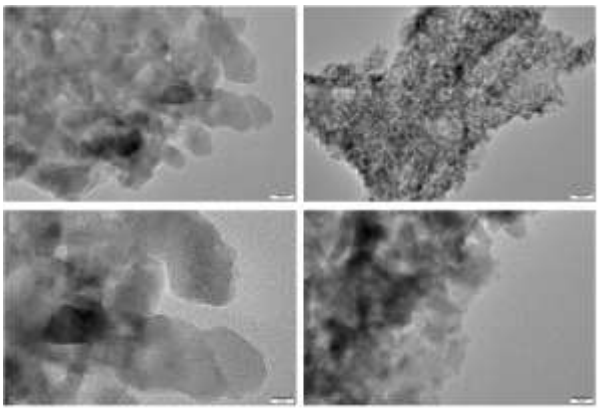

FIGURE 5: TEM images characterizations of as-synthesized C,N-TiO_2

• C,N-TiO_2-Ag Nanocomposite Characterization

The synthesized nanocomposite (C,N-TiO_2-Ag) was characterized via scanning electron microscopy (SEM) and transmission electron microscopy (TEM). The SEM characterization images showed that the nanocomposite displayed a unique lamellar structure form constituted of multiple horizontal layers displayed on its surface. As shown in (figure 6) the layers are horizontal and displayed on the nanocomposite's structure. The TEM results also show the nanocomposite has multiple lamellar layers that are in good agreement with the SEM images. The average size was about 20 nm to 100 nm and had a lamellar layered structure (figure 7).

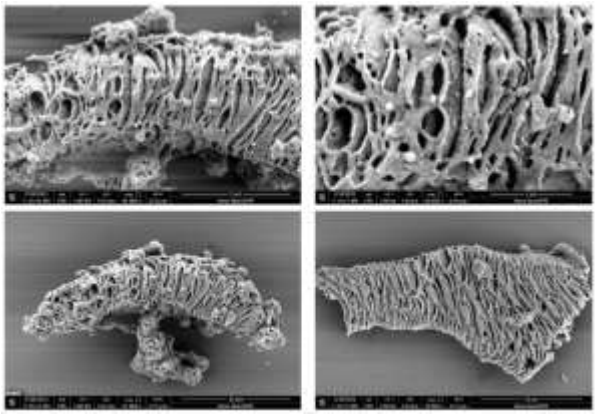

FIGURE 6: SEM characterizations images of C,N-TiO_2-Ag nanocomposite.

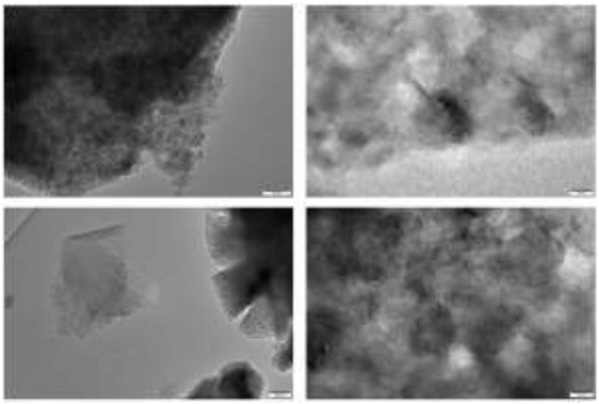

FIGURE 7: SEM characterizations images of C,N-TiO_2-Ag nanocomposite.

To confirm the synthesized nanoparticles obtained crystal structure and purity, X-ray diffraction (XRD) was performed. For the XRD results, if the material is crystal, this can only mean the atoms are arranged in a periodic pattern of three dimensions. The XRD patterns for the C,N-TiO_2 agree with the tetragonal structure of anatase TiO_2, which are in good accordance with the results published by the international center for diffraction data (ICDD). The XRD results clearly showed that the C,N-TiO_2 films annealed at 450 °C revealed the formation of tetragonal anatase TiO_2. The TiO_2 films showed several diffraction peaks at 2θ = 25.355°, 37.842°, 48.141°, 53.945°, 55.183°, 62.810°, and 68.872° were indexed as (101), (004), (200), (105), (211), (204), and (116) respectively. In the same vein, the peaks for the nanocomposite C,N-TiO_2-Ag, results revealed that all the pure titanium dioxide peaks exist. Nevertheless, there was a peak of 2ɵ=27.43 in which represents the rutile (110) crystalline structure exists (figure 8) [19].

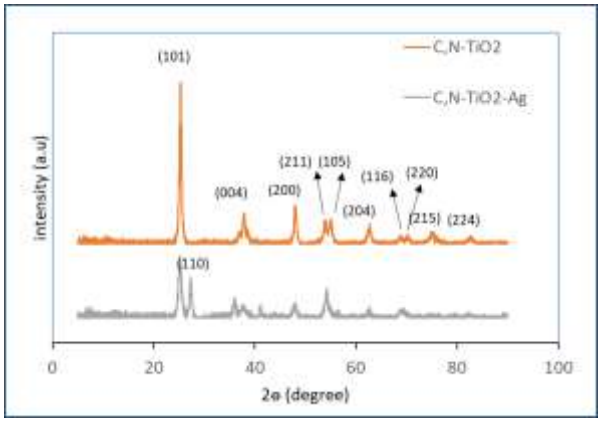

FIGURE 8: XRD characterizations of different synthesized C,N-TiO_2, and C,N-TiO_2-Ag nanoparticles.

- **Bactericidal Activity Assessment**

For decades, TiO_2 has proven to be the most widely used semiconductor metal oxide photocatalyst due to its strong oxidizing effect, biocompatibility, long-term photostability, and low cost. The pure TiO_2 photocatalyst is widely known as an effective agent against Gram-positive and Gram-negative bacteria upon UV irradiation [20] [21]. However, the UV energy doses required to promote adequate sterilization are at levels hazardous to human cells and tissues [22]. For this matter, several approaches were conducted to re-engineer and extend the vast bandgap of TiO_2 toward the photocatalyst's light absorption into the visible range by using transition metals such as silver or non-metal ions (nitrogen or carbon).

In the same vein, it was proved that doping of TiO_2 with nitrogen, and carbon or combined with silver nanoparticles [23] [24] resulted in absorption extending well into the visible range of wavelengths above-mentioned the introduction part. Extending absorption in the visible spectrum of wavelengths was mentioned to be dose-dependent [25].

The minimum inhibitory concentration is the lowest concentration (in µg/mL) of an antibiotic or a chemical that will inhibit the growth of a given strain of bacteria. The MIC was calculated using the agar diffusion method. The bacterial solutions were incubated in the shaker under 180 rpm and 37ºC. after 24h the bacterial solution was taken and diluted via sample and serial dilution. The MIC and MBC of green synthesized AgNPs were done using the method described in the guideline of CLSI, 2012. Small concentrations were prepared to examine their effect on the bacterial samples (E, coli, and B. subtilis), the bacterial samples were placed into 96-well plates to grow under 37°C and continuous shaking at 180 rpm.

DETERMINATION OF MIC AND MBC CONCENTRATION

The MIC test was performed on a 96-well plate using standard broth microdilution methods while the MBC test was performed on the prepared agar plates. The bacterial inoculums were adjusted to the concentration of 10^4 CFU/ml. For the MIC test, 80 µl of the synthesized nanoparticles stock solution was added and diluted twofold with 40 µl bacterial inoculums in 80 µl of the LB started from column 12 to the third column. Column 12 of the microtiter plate contained the highest concentration of AgNPs, C,N-TiO_2 and C,N-TiO_2-Ag nanoparticles while column 3 contained the lowest concentration and column 12 was having the highest concentration of the nanoparticles. The first column served as negative control (only medium) and the second column served as the positive control (medium and bacterial inoculums). Each well of the microtiter plate was added with 80 µl of the Luria Bertani (LB) and incubated at 37°C for 24 h. the inhibition effect of the antibacterial agents was observed as small circles around the wells on the agar as shown on (figure 9). The MIC value was taken at the lowest concentration of antibacterial agents that inhibits the growth of bacteria as shown in (table 1).

The minimum inhibitory concentration was calculated using the same above-mentioned method for calculating the MBC. The MBC is the lowest concentration of a chemical, usually a drug, which prevents the visible growth of a bacterium organism or bacteria. Firstly, the MBC test was performed by plating the suspension from each well of microtiter plates into LB solution plate (figure 9). The plates were incubated at 37°C for 24 h. The lowest concentration with no visible growths on the agar plates was taken as MBC value as we can see in (table 2).

TABLE 1: The MIC values of nanoparticles against E. coli and B. subtilis

Nanoparticles	The MIC values Bacteria	
	E. coli	**B. subtilis**
AgNPs	5 µl/ml	4.8 µl/ml
C,N-TiO_2NPs	5.5 µl/ml	5.7 µl/ml
C,N-TiO_2-Ag nanocomposite	4.1 µl/ml	4.3 µl/ml

TABLE 2: The MBC values of nanoparticles against E. coli and B. subtilis

Nanoparticles	The MIC values Bacteria	
	E. coli	B. subtilis
AgNPs	6.1 µl/ml	6 µl/ml
C,N-TiO_2NPs	7 µl/ml	7.3 µl/ml
C,N-TiO_2-Ag nanocomposite	4.8 µl/ml	5.2 µl/ml

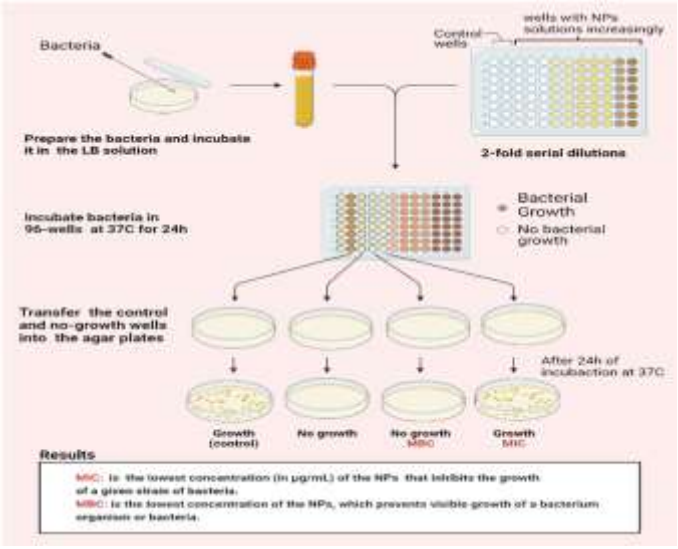

FIGURE 9: MIC and MBC procedures demonstration

Herein, the nanoparticles used in this research have shown promising antibacterial activity. All AgNPs, C,N-TiO_2 and C,N-TiO_2-Ag nanocomposite were investigated against gram-positive (B. subtilis) and gram-negative (E. coli) bacteria. It was found that both microorganisms were found susceptible to the synthesized nanoparticles.

TiO_2 nanoparticles are an exceptional semiconductor material that has been commonly used as an effective antibacterial for self-disinfection and washing. This semiconductor, also known as titania, has unique hydrophilic and photocatalytic characteristics that have extraordinary antibacterial effects against a wide variety of infectious bacteria. The antibacterial activity of the synthesized C,N-TiO_2 nanoparticles, as we can observe in (figure 10) that the C,N-TiO_2 nanoparticles generated good antibacterial activity on both E. coli and B. subtilis bacteria. On the highest concentrations (100ppm) of C,N-TiO_2, the antibacterial activity against gram-negative and gram-positive bacteria was remarkably observed to be increased after 24 hours of incubation, the inhibition rate reached 75%, and 71.2% on E. coli and B. subtilis respectively.

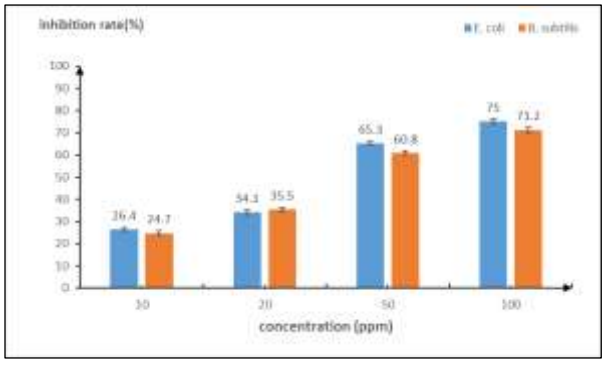

FIGURE 10: Antibacterial effect of C,N-TiO_2 against B. subtilis and E. coli bacteria.

For the synthesized silver nanoparticles (AgNPs), the antibacterial activity was significantly good and promising, silver nanoparticles generated a higher inhibition rate on both bacteria. As stated earlier, AgNPs behavior damages bacterial membrane based on their size and structure, causing reactive oxygen species to be released, creating free radicals with a strong antibacterial activity [26]. For the synthesized silver nanoparticles (AgNPs), the antibacterial activity was significantly excellent and promising. Silver nanoparticles generated a higher inhibition rate on both bacteria. As previously reported, the AgNPs' activity strongly damaged the bacteria membranes depending on the size and shape, which induced reactive oxygen species release forming free radicals with a decisive bactericidal action [26]. In this study, we used the size of about 20 nm with a spherical shape. From (figure 11), we can observe that the AgNPs exhibited a vigorous antibacterial activity on both bacteria, up to 84% and 88.3% of inhibition rate on E. coli and B. subtilis, respectively.

It was also observed that E. coli bacteria were more susceptible to AgNPs than B. subtilis bacteria. It was clear that both gram-negative and gram-positive bacteria growth were inhibited by the synthesized silver nanoparticles. However, the gram-negative (E. coli) bacteria were more susceptible and vulnerable in most cases during all the tests used in this study, starting with the lowest concentration (10ppm), E. coli registered 27.1% compared to 24.8% for B. subtilis and the same case for other concentrations (20, and 50ppm) where E. coli was more inhibited. This strong bactericidal effect of silver against gram-negative bacteria has been explained in many previous studies, it is often related to the thin cell membrane that gram-negative bacteria have and it is easy for Ag^+ ions to penetrate and damage its interior membrane and structure leading to bacterial death.

Unexpectedly, at the highest concentration (100ppm), the B. subtilis was more susceptible and registered 88.3% of the inhibition rate compared to 84% for E. coli. This can be explained by the strong antibacterial activity of AgNPs that can inhibit bacterial growth even for gram-positive bacterial which are known to have a strong and thick cell-wall structure, the accumulation of silver nanoparticles outside the cell-wall of gram-positive bacteria, and the continuous release of Ag^+ ions which work mainly in interrupting the cell-wall exchange of ions and then the ROS including H_2O_2, O_2, and H_2 that can penetrate the cell-wall of bacteria and damage its interior membrane will eventually lead to the cell death. It is also noteworthy to mention that the shape of nanoparticles plays a significant role in their antibacterial activity excellence. Indeed, it was reported that silver nanoparticles with a spherical shape are considered one of the best antibacterial agents. As the spherical shape of nanoparticles is easy to penetrate and pass through the cell wall of the bacteria. It was reported in many previous reports that silver with a spherical shape is more toxic to the bacteria than other nanoparticles with different shapes.

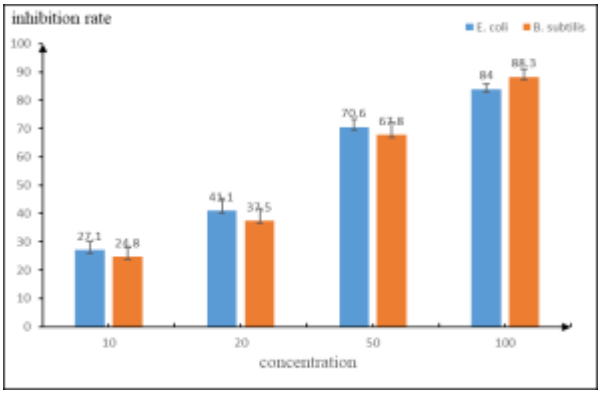

FIGURE 11: Antibacterial effect AgNPs against B. subtilis and E. coli bacteria.

Furthermore, to examine the efficiency of novel synthesized nanocomposite (C,N-TiO_2-Ag), we kept the same experimental conditions as used in assessing the antibacterial activity of both C,N-TiO_2, and AgNPs nanoparticles. The synthesis method that we used has significantly increased the antibacterial activity of titanium dioxide and silver nanoparticles against the bacteria. The nanocomposite showed a substantial and maximum antibacterial effect on E. coli compared to B. subtilis bacteria for most used doses. For the highest dose used in this study (100ppm) the inhibition rate reached 91.1% and 94.8% against B. subtilis and E. coli, respectively. Also, it was observed that the effect is dose-dependent, more we increased the nanocomposite concentration, more the effect was significantly higher (figure 12). We can observe that in all concentrations used in this test the E. coli (gram-negative) was most inhibited by the nanocomposite, at 10ppm only the inhibition rate was around 37.9% compared to 34.8% for B. subtilis, and so on or the other concentration, the inhibition rate values reveal that E. coli was most vulnerable to the nanocomposite solution than B. subtilis, even with the highest concentration the E. coli remains the most susceptible bacteria with an inhibition rate reached 94.8% against E. coli and 91.1% against b. subtilis. The E. coli bacteria with its thin cell-wall membrane was very susceptible to the strong synergistic effect of AgNPs and TiO_2 together. The strong inhibition rate, can be explained by the synergistic effect of AgNPs and TiO_2, when the AgNPs interact with the TiO_2 NPs the photocatalytic activity of titanium dioxide increases intensely which is very toxic to bacteria particularly gram-negative bacteria, and the release of reactive oxygen species is very high.

This nanocomposite is a promising antibacterial agent because it includes two of the strongest bactericidal agents without the use of UV light irradiation. It has proved that the use of UV light to activate the photocatalytic effect of TiO_2 is no longer necessary and the synergistic effect between these two materials can be improved more for future utilizations. Also, we observed that the effect of this nanocomposite is following the dose-dependent pattern, after the analysis of the figures (10, 11, and 12) results. Comparing the three nanoparticles' effect on both bacteria, we can conclude that the nanocomposite had the highest and the better activity on both microorganisms used in this study. These results demonstrate that the doping method has shown a good enhancement of the antibacterial activity against both bacterial species, making it very promising to be used as a new disinfecting tool for many applications in different domains.

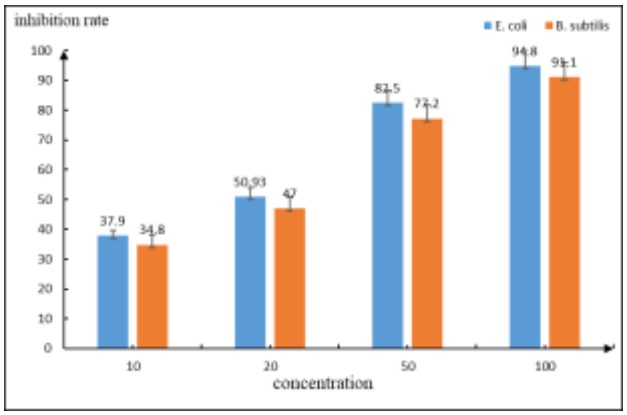

FIGURE 12: Antibacterial effect of the nanocomposite C,N-TiO_2-Ag on E. coli and B. subtilis.

Undeniably, all nanomaterials' antibacterial activity in this study on both bacteria was significant and promising, with some slight difference of effect between E. coli and B. subtilis. As we observed that E. coli growth was the most influenced and inhibited by the concentration of dispersed nanoparticles, while B. subtilis was the lowest affected by these nanoparticles. These results could be accredited due to gram-positive bacteria (B. subtilis) has a more robust molecular system in the cell wall than gram-negative bacteria (E. coli). Indeed, its thin membrane carries a negative charge that makes it easier to penetrate and destroy Ag^+ and ROS generated by nanoparticles under light irradiation, which allows the ions to penetrate the cell walls of gram-negative easier than entering the cell walls of gram-positive bacteria. It is well known that gram-negative bacteria have a single thin peptidoglycan layer and an outer membrane, unlike gram-positive bacteria that have multiple thick peptidoglycan layers and a thick cell wall. Therefore, in gram-positive organisms, the generated oxidant species must pass by the multiple peptidoglycan layers which are composed of complex layers of lipids, lipopolysaccharide, and proteins, that makes it complicated for nanoparticles to reach the thick cell-wall then to the cytoplasmic membrane and damage the cell as previously reported by [27].

Moreover, it's also worth mentioning that this antibacterial activity is dose-dependent; the more we increased the nanocomposite concentration, the more the bacterial concentrations were decreased significantly. For instance, during the reaction of the reduction of ions (Ag^+) to silver nanoparticles, Ag^+ will be associated with an (NADH) dependent reductase enzyme production as a secondary metabolite, as it was determined in a preliminary protein assay of silver nanoparticle formation by Fusarium oxysporum in a study done by [28].The nanoparticles' reactions with bacteria put it in the exposure to reactive intermediates that transferred from the surface of AgNPs, C,N-TiO_2, and C,N-TiO_2-Ag coatings to the outside of the bacteria, such as superoxide anions (O_2), hydrogen peroxide (H_2O_2), and hydroxyl radicals (•OH), whose can damage the bacterial proteins, nucleic acids, etc. In addition, the initial attack takes place on the cell wall, where the bactericide makes the first contact with an intact bacterium [29]. Damages on bacterial cell wall will lead to the perturbation of different cellular processes, and then the leakage of the cytoplasm, finally bacteria inactivation and death [30].

CONCLUSIONS AND FUTURE PERSPECTIVES

In the current study AgNPs, C,N-TiO_2, and C,N-TiO_2-Ag nanocomposite synthesis and their antibacterial activity against both gram-positive and gram-negative bacteria were successfully achieved and well investigated. This study showed the effectiveness of the synthesis methods of different nanoparticles AgNPs, C,N-TiO_2, and C,N-TiO_2-Ag nanocomposite and its importance in creating a new and promising antibacterial agent. This combination approach has shown to be most promising in terms of the increase of the absorption range of TiO_2 nanoparticles into the visible light area to increase the photocatalytic activity of titanium dioxide nanoparticles and enhanced the antibacterial effect. It also presents an alternative way to avoid UV light irradiation to activate the titanium dioxide nanoparticles, which were already reported to be harmful to human health. The synthesized nanoparticles used in this study have shown an excellent antibacterial effect against both bacterial strains used in this study. Particularly, the novel synthesized nanocomposite reached up to 94% and 91.1% of inhibition rate on E. coli and B. subtilis, respectively.

This study paves the way for research in new technology (nanotechnology) to battle bacterial infections.

However, it comes up with its drawbacks. To name but a few; the different sizes and shapes of nanomaterials, the study used only two bacteria (E. coli and B. subtilis), and this stopped at the level of lab experiments didn't use any food packaging or water treatment experiments etc.

REFERENCES

[1] Siegel RE. Emerging gram-negative antibiotic resistance: Daunting challenges, declining sensitivities, and dire consequences. Respiratory Care 2009; 53(4): 471–9.

[2] Sirelkhatim A, Mahmud S, Seeni A, *et al.* Review on zinc oxide nanoparticles: Antibacterial activity and toxicity mechanism. Nano-Micro Letters 2015; 7(3): 219–42 [https://doi.org/10.1007/s40820-015-0040-x]

[3] Sharma D, Kanchi S, Bisetty K. Biogenic synthesis of nanoparticles: A review. Arabian Journal of Chemistry 2019; 12(8): 3576–600 [https://doi.org/10.1016/j.arabjc.2015.11.002]

[4] Matsunaga T, Tomoda R, Nakajima T, Wake H. Photoelectrochemical sterilization of microbial cells by semiconductor powders. FEMS Microbiol Lett 1985; 29(1-2): 211–4 [https://doi.org/10.1111/j.1574-6968.1985.tb00864.x]

[5] Hoffmann MR, Martin ST, Choi W, Bahnemann DW. Environmental Applications of Semiconductor Photocatalysis. Chemical Reviews 1995; 95(1): 69–96 [https://doi.org/10.1021/cr00033a004]

[6] Linsebigler AL, Lu G, Yates Jr JT. Photocatalysis on TiO2 surfaces: principles, mechanisms, and selected results. Chemical Reviews 1995; 95(3): 735–58.

[7] Sukdeb Pal, Yu Kyung Tak, Joon Myong Song. Does the Antibacterial Activity of Silver Nanoparticles Depend on the Shape of the Nanoparticle? A Study of the Gram-Negative Bacterium Escherichia coli. Appl. Environ. Microbiol. 2007; 73(6): 1712–20 [https://doi.org/10.1128/AEM.02218-06] [PMID: 17261510]

[8] Gerischer H, Heller A. The role of oxygen in photooxidation of organic molecules on semiconductor particles. Journal of Physical Chemistry 1991; 95(13): 5261–7 [https://doi.org/10.1021/j100166a063]

[9] Rothenberger G, Moser J, Graetzel M, Serpone N, Sharma DK. Charge carrier trapping and recombination dynamics in small semiconductor particles. Journal of the American Chemical Society 1985; 107(26): 8054–9 [https://doi.org/10.1021/ja00312a043]

[10] Jiang R, Li B, Fang C, Wang J. Metal/semiconductor hybrid nanostructures for plasmon-enhanced applications. Advanced Materials 2014; 26(31): 5274–309 [https://doi.org/10.1002/adma.201400203]

[11] Kohno Y, Hayashi H, Takenaka S, Tanaka T, Funabiki T, Yoshida S. Photo-enhanced reduction of carbon dioxide with hydrogen over Rh/TiO2. Journal of Photochemistry and Photobiology A: Chemistry 1999; 126(1): 117–23 [https://doi.org/10.1016/S1010-6030(99)00113-6]

[12] Liu Y, Wang X, Yang F, Yang X. Excellent antimicrobial properties of mesoporous anatase TiO2 and Ag/TiO2 composite films. Microporous and Mesoporous Materials 2008; 114(1): 431–9 [https://doi.org/10.1016/j.micromeso.2008.01.032]

[13] Li P, Li J, Wu C, Wu Q, Li J. Synergistic antibacterial effects of β-lactam antibiotic combined with silver nanoparticles. Nanotechnology 2005; 16(9): 1912–7 [https://doi.org/10.1088/0957-4484/16/9/082]

[14] Meng XK, Tang SC, Vongehr S. A Review on Diverse Silver Nanostructures. Journal of Materials Science and Technology 2010; 26(6): 487–522 [https://doi.org/10.1016/S1005-0302(10)60078-3]

[15] Liu SX, Qu ZP, Han XW, Sun CL. A mechanism for enhanced photocatalytic activity of silver-loaded titanium dioxide. Catalysis Today 2004; 93-95: 877–84 [https://doi.org/10.1016/j.cattod.2004.06.097]

[16] Seery MK, George R, Floris P, Pillai SC. Silver doped titanium dioxide nanomaterials for enhanced visible light photocatalysis. Journal of Photochemistry and Photobiology A: Chemistry 2007; 189(2): 258–63 [https://doi.org/10.1016/j.jphotochem.2007.02.010

[17] Akhavan O. Lasting antibacterial activities of Ag–TiO2/Ag/a-TiO2 nanocomposite thin film photocatalysts under solar light irradiation. J Colloid Interface Sci 2009; 336(1): 117–24 [https://doi.org/10.1016/j.jcis.2009.03.018]

[18] Ni C, Hassan PA, Kaler EW. Structural characteristics and growth of pentagonal silver nanorods prepared by a surfactant method. Langmuir 2005; 21(8): 3334–7 [https://doi.org/10.1021/la046807c] [PMID: 15807571]

[19] Suwarnkar MB, Dhabbe RS, Kadam AN, Garadkar KM. Enhanced photocatalytic activity of Ag doped TiO2 nanoparticles synthesized by a microwave assisted method. Ceramics International 2014; 40(4): 5489–96 [https://doi.org/10.1016/j.ceramint.2013.10.137]

[20] Foster HA, Ditta IB, Varghese S, Steele A. Photocatalytic disinfection using titanium dioxide: spectrum and mechanism of antimicrobial activity. Applied Microbiology and Biotechnology 2011; 90(6): 1847–68.

[21] Cai Y, Strømme M, Welch K. Photocatalytic Antibacterial Effects Are Maintained on Resin-Based TiO2 Nanocomposites after Cessation of UV Irradiation. PLoS ONE 2013; 8(10) [https://doi.org/10.1371/journal.pone.0075929]

[22] Musk P, Campbell R, Staples J, Moss DJ, Parsons PG. Solar and UVC-induced mutation in human cells and inhibition by deoxynucleosides. Mutation Research Letters 1989; 227(1): 25–30 [https://doi.org/10.1016/0165-7992(89)90064-X]

[23] Gamage McEvoy J, Cui W, Zhang Z. Degradative and disinfective properties of carbon-doped anatase-rutile TiO2 mixtures under visible light irradiation. Catalysis Today 2013; 207: 191–9 [https://doi.org/10.1016/j.cattod.2012.04.015]

[24] Asahi R, Morikawa T, Ohwaki T, Aoki K, Taga Y. Visible-light photocatalysis in nitrogen-doped titanium oxides. Science 2001; 293(5528): 269–71 [https://doi.org/10.1126/science.1061051]

[25] Jagadale TC, Takale SP, Sonawane RS, *et al.* N-Doped TiO2 Nanoparticle Based Visible Light Photocatalyst by Modified Peroxide Sol–Gel Method. The Journal of Physical Chemistry C 2008; 112(37): 14595–602 [https://doi.org/10.1021/jp803567f]

[26] Wu D, Fan W, Kishen A, Gutmann JL, Fan B. Evaluation of the Antibacterial Efficacy of Silver Nanoparticles against Enterococcus faecalis Biofilm. Journal of Endodontics 2014; 40(2): 285–90 [https://doi.org/10.1016/j.joen.2013.08.022]

[27] Page K, Palgrave RG, Parkin IP, Wilson M, Savin SLP, Chadwick AV. Titania and silver-titania composite films on glass - Potent antimicrobial coatings. J. Mater. Chem. 2007; 17(1): 95–104 [https://doi.org/10.1039/b611740f]

[28] Ahmad, A., Mukherjee, P., Senapati, S., Mandal, D., Khan, M. I., Kumar, R., & Sastry, M. Extracellular biosynthesis of silver nanoparticles using the fungus Fusarium oxysporum. Colloids and Surfaces B: Biointerfaces 2003; 4(28): 313–8.

[29] Halliwell B, Gutteridge JMC. Free Radicals in Biology and Medicine. Oxford University Press 2015.

[30] Lonnen J, Kilvington S, Kehoe SC, Al-Touati F, McGuigan KG. Solar and photocatalytic disinfection of protozoan, fungal and bacterial microbes in drinking water. Water Research 2005; 39(5): 877–83 [https://doi.org/10.1016/j.watres.2004.11.023]